

An automatic skateboarder detection method with roadside LiDAR data

Jianqing Wu, Hao Xu, Rui Yue, Zong Tian, Yuan Tian & Yuxin Tian

To cite this article: Jianqing Wu, Hao Xu, Rui Yue, Zong Tian, Yuan Tian & Yuxin Tian (2019): An automatic skateboarder detection method with roadside LiDAR data, Journal of Transportation Safety & Security, DOI: [10.1080/19439962.2019.1633573](https://doi.org/10.1080/19439962.2019.1633573)

To link to this article: <https://doi.org/10.1080/19439962.2019.1633573>



Published online: 02 Jul 2019.



Submit your article to this journal [↗](#)



Article views: 26



View Crossmark data [↗](#)



An automatic skateboarder detection method with roadside LiDAR data

Jianqing Wu , Hao Xu, Rui Yue, Zong Tian, Yuan Tian, and Yuxin Tian

Department of Civil and Environmental Engineering, University of Nevada, Reno, NV, USA

ABSTRACT



The increasing conflicts between skateboarders and pedestrians on the campuses have caused safety concerns. Although traffic planners on campus usually did not consider skateboarding into planning due to the lack of historical skateboarding data. The traditional data collection method such as manual counting or video detection took a lot of effort and could only provide macrolevel skateboarding data. Therefore, this research presented a new approach for skateboarder detection using the roadside LiDAR sensor. A two-stage classification method was developed to distinguish skateboarders and other road users. The first stage was to classify motor vehicles and nonvehicles (pedestrians, bicycles, and skateboarders). Then the second step was to distinguish skateboarders from pedestrians and bicycles. The proposed procedure was evaluated using real-world data on campus. The results showed that the proposed procedure can detect the skateboarder with the overall accuracy of 89.5%. The data collected in the real world showed that the speed of the skateboarder was usually higher than the pedestrian and lower than the bicycle. The skateboarding information extracted from the proposed detection method could be applied for skateboarder behavior analysis, volume counting, and safety analysis. A level-based procedure to reinforce the safety between skateboarders and pedestrians was recommended.

KEYWORDS

Skateboarder; automatic detection; roadside LiDAR; traffic safety

1. Introduction

Skateboarding is a recreational activity which is particularly popular among young people (Fang, 2013). Some people, especially students on the college campus, also use skateboards for travel. Skateboards can be essentially ridden on any paved areas including roads, sidewalks, bike paths, parking lots, pedestrian paths, open plazas, etc. Safety has been a major concern for skateboarding given the reputation of recreational skateboarding as an extreme sport. At least 147 skateboarders were killed in the United States from 2011 to 2015, almost all on roads (Fang & Handy, 2017). Another

CONTACT Rui Yue  ryue@nevada.unr.edu  Department of Civil and Environmental Engineering, University of Nevada, Reno, 1664 N. Virginia Street, MS258, Reno, NV 89557, USA.

© 2019 Taylor & Francis Group, LLC and The University of Tennessee

report from the United States showed that 65% of skateboard-related injuries occurred on public roads, in parking lots, and on footpaths, which were outside of areas designated for skateboarding (Fountain & Meyers, 1996). Although skateboarding is often prohibited in large sections of cities, including roads, sidewalks, districts, and areas of certain land use types (Fang, 2013), it is usually allowed around college campuses. A previous survey (Fang, 2015) showed that about 7% of students used skateboards to reach campus at the University of California, Santa Barbara (UCSB). Skateboarding is famous on campus because students can use skateboards to travel nearly door to door without having to divert to parking lots or bike racks (Fang, 2014). The safety issue related to skateboarding is rigorous on campus considering the heavy student volume between classes and the possible conflicts between skateboarders and pedestrians. Although the speed of skateboarding on roads may not be as high as recreational skateboarding, it is usually much higher than the speed of pedestrians. Furthermore, unsafe skateboard maneuvers can be dangerous. The skateboarders may pass the pedestrians suddenly without any warning, which may cause the pedestrians to feel nervous. A previous survey showed that the pedestrians felt uncomfortable if a skateboarder passed them with relatively high speed (American Academy of Pediatrics, 2002). The wide use of a cell phone when skateboarding further intensified the conflicts between skateboarders and other road users owing to using a cell phone could lead the skateboarders to eye-off-road (Wu & Xu, 2018). Higher risk activities such as sitting on the skateboard to ride downhill on the road or “skitching a ride” behind a moving vehicle also increase the risk of severe or fatal injuries.

Several universities regulate skateboarding with limitations on where students can ride on campus (University of Utah, 2009; University of California San Diego, 1997; Carleton University, 2005). The University of Nevada, Reno (UNR; 2015) is also seeking countermeasures to reduce the conflicts between skateboarders and pedestrians on campus. The campus police continuously received the complaints from students mentioning that they were almost hit by skateboarders. The current skateboarding activities are unsafe and require further investigation, which is very important for traffic planners and decision makers, especially for those on college campuses. However, it is not easy to perform a safety evaluation related to skateboarders due to the limited data. For historical crash data, the skateboarders were usually considered as the pedestrians by the police and were often classified as road casualties in the traffic crash database (Nevada Traffic Crash Database, 2009). Because the frequency of crashes involving skateboarders was lower compared to other crash types (Inoue, Barker & Scott, 2009), previous efforts (Lustenberger & Demetriades, 2017; Porter,

Neto, Balk & Jenkins, 2016) usually focused on analyzing skateboarding activities, such as counting skateboarder volume, analyzing moving direction and speed through the field collected data. The most widely used data collection method in the field was camera detection technology. Although a lot of image-processing technologies can automatically extract moving objects from the videos (Malinovskiy, Wu, & Wang, 2008; Ren et al., 2016; Hoogendoorn, Daamen, & Bovy, 2003), it was still difficult to distinguish skateboarders and pedestrians through image-based technologies. Furthermore, the performance of image-based technologies was always affected by lighting conditions (Wu, Xu, Zhao, & Simpson, 2018). Manually counting skateboarder volume was another option but could be time-consuming for long-term data collection. In addition, the speed of skateboarder can only be roughly estimated with manual counting method. A lot of studies have been conducted for pedestrian detection and counting using radar sensors or passive infrared counters. For example, Milch and Behrens (2001) used on-board radars and cameras to detect pedestrians. Beckwith and Hunter-Zaworski (1998) applied the Droppler radar for pedestrian detection. The testing results showed that the radar can detect pedestrians at a distance of 9.1 m (30 ft) with high accuracy. Kothuri, Nordback, Schroepe, Phillips, & Figliozi (2017) tested the effectiveness of four technologies for pedestrian counting: inductive loops, thermal cameras, passive infrared counters, and pedestrian actuation data. It was found that passive infrared counters can count pedestrians accurately at the intersection sidewalk. The above-mentioned studies already show that pedestrian detection and counting technologies were mature. So can those technologies be used for skateboarder detection and counting? One of the challenges lies in the classification between pedestrians and skateboarders. Those previous practices usually did not distinguish pedestrians and skateboarders. Moreover, the above-mentioned papers only provided spot detection, meaning only pedestrians located in a small range can be detected. As a result, the trajectories of skateboarders could not be extracted using the above-mentioned technologies. Therefore, it is necessary to explore a new method for automatic skateboarder detection.

The 360° light detection and ranging (LiDAR) technology can provide the 3D point cloud for the surrounding objects, which may provide a solution for skateboarder detection. The LiDAR is a surveying method that measures the distance to a target by illuminating the target with pulsed laser light and measuring the reflected pulses with a sensor. With the LiDAR sensor deployed along the roadside, the LiDAR sensors can generate the point cloud for each road users, including vehicles, pedestrians, skateboarders, etc. The roadside LiDAR mentioned here worked in a different situation compared to the airborne LiDAR and the on-board LiDAR.

Airborne LiDAR has been widely used for remote-sensing applications, such as forest investigations, digital elevation models (DEMs), generation etc. (Yang, Fang, & Li, 2013). LiDAR technology is also used in control and navigation for autonomous vehicles, which is called “on-board LiDAR” (Li, Zheng, & Cheng, 2004). The autonomous vehicles use the on-board LiDAR (usually working together with cameras) to detect road boundaries, pedestrians, vehicles, and obstacles. Different from the airborne LiDAR and the on-board LiDAR, the roadside LiDAR works in a relatively static situation (Wu, Xu, & Zheng, 2017). The authors have developed a series of data processing algorithms for roadside LiDAR sensors, covering different aspects-background filtering (Wu, Xu, & Zheng, 2017; Wu, Xu, Sun, Zheng, & Yue, 2018; Wu, Tian, Xu, Yue, Wang, & Song, 2019), lane identification (Wu, Xu, & Zhao, 2019; Zhao, Xu, Wu, & Liu, 2018), object classification (Sun, Xu, Wu, Zheng, & Dietrich, 2018), vehicle tracking (Wu, 2018), and data broadcasting (Zheng, Xu, Tian, & Wu, 2018). Those preliminary works provide the basis for the skateboarder detection using the roadside LiDAR.

This paper presents a procedure and related methods to detect skateboard with a roadside LiDAR sensor. The procedure includes four major parts: background filtering, object clustering, object tracking, and object classification. The effectiveness of this procedure is evaluated using field collected data. The skateboard volume, speed, trajectories, and crucial events can be extracted from roadside LiDAR data. This paper is structured as follows: Section 2 documents the procedure of roadside data collection and the method for skateboard detection. Section 3 uses the case study to evaluate the proposed method. In Section 4, skateboarder behavior analysis is presented. Section 5 summarizes the major contribution of this research and future extension.

2. Roadside LiDAR data collection and data processing

2.1. Roadside LiDAR

The roadside LiDAR sensor can be temporarily installed on a tripod for a pilot study or permanently installed on the roadside structures for the long-term data collection. The location of the installation should allow the LiDAR to detect the objects on the road as far as possible. The location of the LiDAR should also consider the possible human destroy. The suitable position of the LiDAR could be on the top of a pedestrian signal or the similar height on the wire pole. Considering the different parameters of different LiDAR sensors, the location for installation should also be different. In this paper, we used the VLP-16 LiDAR sensor for data collection. The primary reason for selecting the VLP-16 is that the price of this LiDAR

Table 1. Parameters of VLP-16

Rotation rate	5 Hz–20 Hz	Field of view (vertical)	+15.0° to –15.0°
Weight	830 g	Field of View (Horizontal)	360°
Dimensions	103 mm diameter × 72 mm height	Wavelength	903 nm
Measurement range	Up to 100 m	Channels	16
Operating temperature	–10 °C to +60 °C	Accuracy	±3 cm

sensor is relatively low, which is acceptable for practical applications. Another reason is that the VLP-16 is a 360° LiDAR sensor, which can cover the whole lateral area on the road. The detailed parameters of VLP-16 are documented in Table 1.

The VLP-16 reports coordinates of all scanned points in spherical coordinates (r, ω, α), which are converted into Cartesian coordinates (x, y, z) automatically by the sensor. Based on the GPS location of the LiDAR, all the points can be matched to the exact location in the real world. In this research, we deployed the LiDAR on a tripod (about 5 ft above the ground) for the temporary data collection. Figure 1 shows an example of a portable LiDAR installation.

2.2. Background filtering

The background can be buildings and ground surface, as well as moving objects such as waving trees and bushes. The locations of these dynamic background objects (waving trees and bushes) are not stationary. Even for the stationary background points, their locations and number of points are not the same in different frames because of LiDAR vibration or blocking of moving objects. The background filtering algorithm needs to exclude the background points as much as possible and keep the vehicle points at the same time. A background filtering method named 3D density statistic filtering (3D-DSF) was developed by the authors (Wu, Xu, Sun, Zheng, & Yue, 2018) to exclude the background automatically, which is briefly introduced as follows. The 3D-DSF algorithm firstly collects raw data in a period as the initial input. The raw data are then aggregated into one 3D space based on their coordinates. The recommended number of frames for aggregation is between 1500 and 3000 considering the accuracy and the time cost. The 3D space is then divided into multiple cubes for density statistics. Each cube can be identified as a background space or not based on the point density in each cube. Compared to the background points, the number of moving vehicle points is fewer. Therefore the background space can be identified by giving an appropriate threshold. The thresholds should be different with different sites and vary with the number of objects in the aggregated frames. A detailed automatic threshold learning was documented by authors in (Wu, Xu, Sun, Zheng, & Yue, 2018). The location of the background can then be stored in a background profile (3D matrix).



Figure 1. Portable Light Detection and Ranging (LiDAR)

For real-time data processing, the points in each frame are firstly transferred into a 3D matrix and then compared with the location of the background profile. Any point found in the location of the background profile is then excluded from the database. After getting the background location profile, the time needed to exclude background for the real-time task is about 100 ms, which is enough to serve the real-time data processing task. Figure 2 shows an example of LiDAR data before-and-after background filtering. The further before-and-after evaluation shows that the algorithm can exclude more than 97% of background points, and keep about 98% of vehicle points at the same time.

2.3 Object clustering

After background filtering, points belonging to one vehicle need to be clustered into one group. Density-based clustering is very suitable for vehicle clustering in LiDAR data as the point density of vehicles is much higher compared with other areas in the space. Density-based spatial clustering of applications with noise (DBSCAN) is one of the most popular density-based clustering algorithms (Zhao, Xu, Liu, Wu, Zheng, & Wu, 2019). The DBSCAN is very effective to cluster density-related points in the space. Another advantage of DBSCAN is that the algorithm does not need to know how many objects are on the road. The DBSCAN algorithm requires two parameters, epsilon (ϵ), which specifies how close points should be to each other to be considered a part of a cluster; and a minimum number of points (MinPts), which specifies how many neighbors a point should have to be included into a cluster. The detailed introduction about the parameters selection can be found in Zhao, Xu, Wu, & Liu (2018).

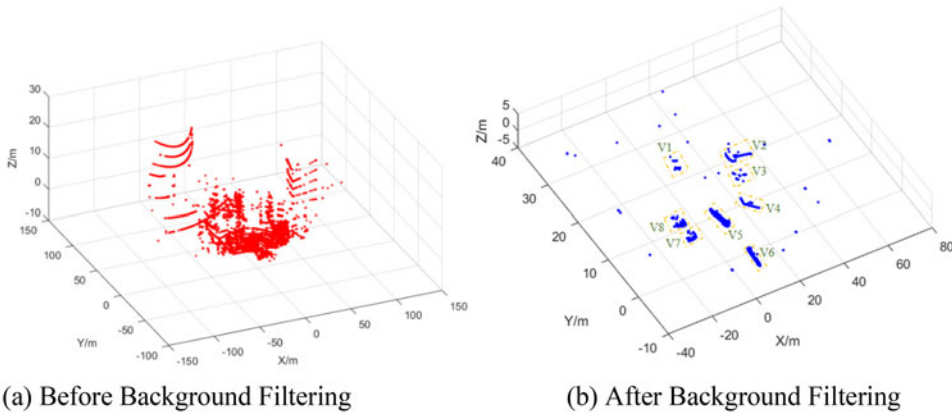


Figure 2. Background filtering with 3D-DSF

2.4 Object tracking

To continuously track the same object, the same object in different frames needs to be associated. The nearest neighbor (NN) algorithm was applied to associate the same object in different frames (Wu, 2018). The idea of the NN is that an object in the current frame is matched to an object in the previous frame if the distance between these two objects is the shortest among all the candidate objects within a certain time period. The candidate objects are selected by the area within the distance threshold. The distance threshold is determined based on the speed limit of the road and the time difference between frames. It should be noted that object association happens in each lane space when there are multiple vehicles in multiple lanes. When an object in the current frame cannot find a matched object in the previous frame, a new tracking ID is assigned. Each tracked object uses the same object ID in different frames. After objects were matched, a discrete Kalman filter tracking method was further used for tracking the objects. The position/speed/acceleration information of the object in the previous frame and the position/speed/acceleration information of the matched object in the current frame were the input of the Kalman filter to estimate the status of the object in the current frame. For some frames where clusters cannot be detected (occlusion or failure of clustering), the Kalman filter can be used to predict the status of the missing object, thus improving the tracking continuity.

2.5 Classification

There may be different road users, such as vehicles, pedestrians, skateboards, bicycles, etc. An example of the shapes of different road users is shown in Figure 3. The shapes of other road users—pedestrians/skateboarders/bicycles were found quite different from that of vehicles. The pedestrian

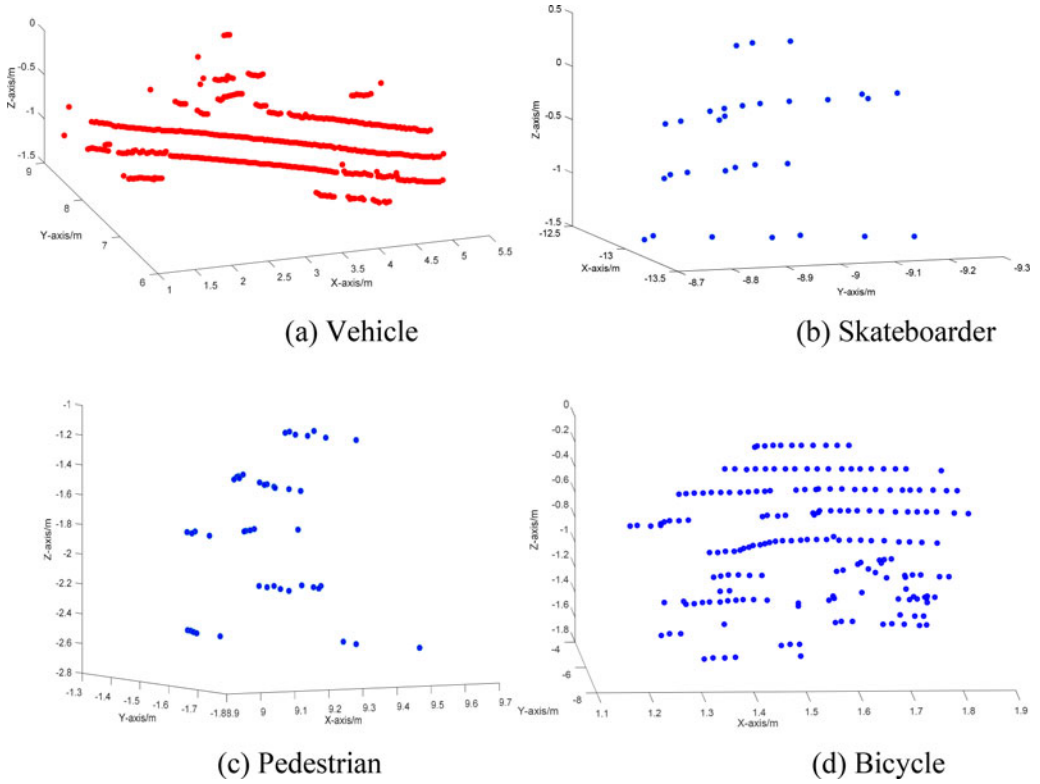


Figure 3. Shapes of different road users

and the skateboarder have the similar shape in LiDAR data. The shape of a bicycle is some different from that of a skateboarder, but the difference is not obvious. As mentioned before, the classification was divided into two stages. The first step was to distinguish vehicles and other road users. And the second step was to distinguish pedestrians, skateboarders, and bicycles.

2.5.1. Vehicle and other users classification

Appropriate features are very pivotal for classification algorithms. Although intensity was also reported in the point cloud, the practice showed that it was unstable and changes between different objects subject to different reflecting strength and the angles between objects to LiDAR (Zhao, Xu, Wu, Zheng, & Liu, 2018). As is shown in Figure 3, the shapes information can be used to distinguish vehicles and other road users. Inspired by the previous work (Lee & Coifman, 2012), this paper considered the following features:

1. Number of points. Usually, the number of points representing vehicles is more than that representing pedestrians/skateboarders/bicycles at the same distance to LiDAR.

2. Distance to LiDAR. For one object, the shape of the object varies with different distances to LiDAR.
3. Object Length. The length of the object was estimated through [equation \(1\)](#):

$$L = \max \left(\sqrt{(X_i - X_j)^2 + (Y_i - Y_j)^2} : i \neq j \right) \quad (1)$$

Where, X_i is the X-axis value of point i and Y_i is the Y-axis value of point i . In [Equation 1](#), the distance between any pair of two different points was calculated. The max distance of two-point-pair was selected to represent the length of the object. (Note: The length calculated here is different from the actual length of the object.)

1. [Aspect ratio](#)-the value of object height divided by object length. Usually, the length of a vehicle is much longer than the height of other road users.

This paper tested the performance of different methods, including [Naïve Bayes](#) (NB) (Huang, Chin, & Haque, 2009), K-nearest neighbor classification (KNN) (Tan, Wang, Wu, Wang, & Pan, 2016), random forest (RF), and support vector machine (SVM) (Chen, Pears, Freeman, & Austin, 2009) for classification.

2.5.2 Skateboarder, pedestrian, and bicycle classification

The second step was to distinguish skateboarders from pedestrians and bicycles. As is shown in [Figure 3](#), it is even difficult to distinguish them by manually reviewing the point cloud. Other than the shape, the speed information can also be used to distinguish those three different groups. [Figure 4](#) shows an example of speed distributions of different road users in the LiDAR data. The speed of the skateboarders were higher than that of the pedestrians but lower than that of the bicycles. The pedestrians usually keep a consistent speed while the speed variance of skateboarding may be higher since the skateboarder needs to thrust against the ground to improve the speed intermittently (American Academy of Pediatrics, 2002).

The following parameters were applied for skateboarder identification.

1. [Average speed in the trajectory](#). Note: The lengths of the trajectories may be different considering the characteristics of different movements.
2. [The standard deviation of speed in the trajectory](#). Note: This parameter is used to reflect the fluctuation of the speed.

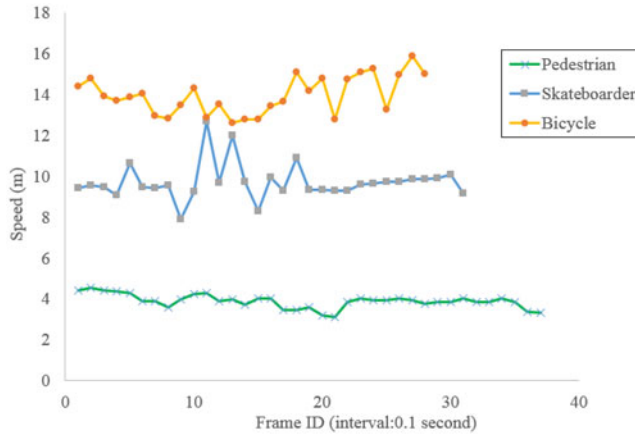


Figure 4. Speed distribution of different road users. Note: The speeds were calculated using the nearest neighbor algorithm in Section 2.4.2.

3. Case study of skateboarder detection

To evaluate the effectiveness of the proposed procedure, four sites on/around the UNR campus were selected to collect the skateboarder data. Figure 5 shows the map of the four sites.

Site 1 is at the corner of the quad. The quad was selected because the campus police received a lot of complaints about the skateboarding with fast speed using this area. Site 2 is at the front of the AB building. There are a lot of classrooms in the AB building, and a lot of skateboarders, bicycles, and pedestrians were observed during the break between classes. Site 3 was at one unsignalized midblock near the Knowledge Center. Students have safety concerns about this midblock due to a steep slope at this site (Wu, Xu, Zheng, & Tian, 2018). Site 4 was selected at the northwestern corner of the Virginia St@15th St. A lot of students cross the intersection of Virginia St@15th St during weekdays. Figure 6 shows the field data collection pictures.

The data at Site 1 were collected at three time windows (7:30 am to 9:00 am, 11:00 am to 1:00 pm, 4:00 pm to 6:00 pm) on April 23, 2018. The data at Site 2 were collected from 7:00 am to 6:00 pm on May 5, 2018. Data at Site 3 were collected from 9:30 am to 1:30 pm on April 5, 2019. And data at Site 4 were collected from 9:00 am to 3:00 pm on April 22, 2019. However, no skateboarders were detected at Site 4 (out of campus).

During the background step, 2000 frames were used for aggregation at each site. Figure 7 shows an example of background filtering results using 3D-DSF at Site 2. The results show that most background points were excluded during the background filtering step and road users were left at the same time. There were three road users including one skateboarder and two pedestrians in the detected range. After applying 3D-DSF, all the road users were kept in the space.

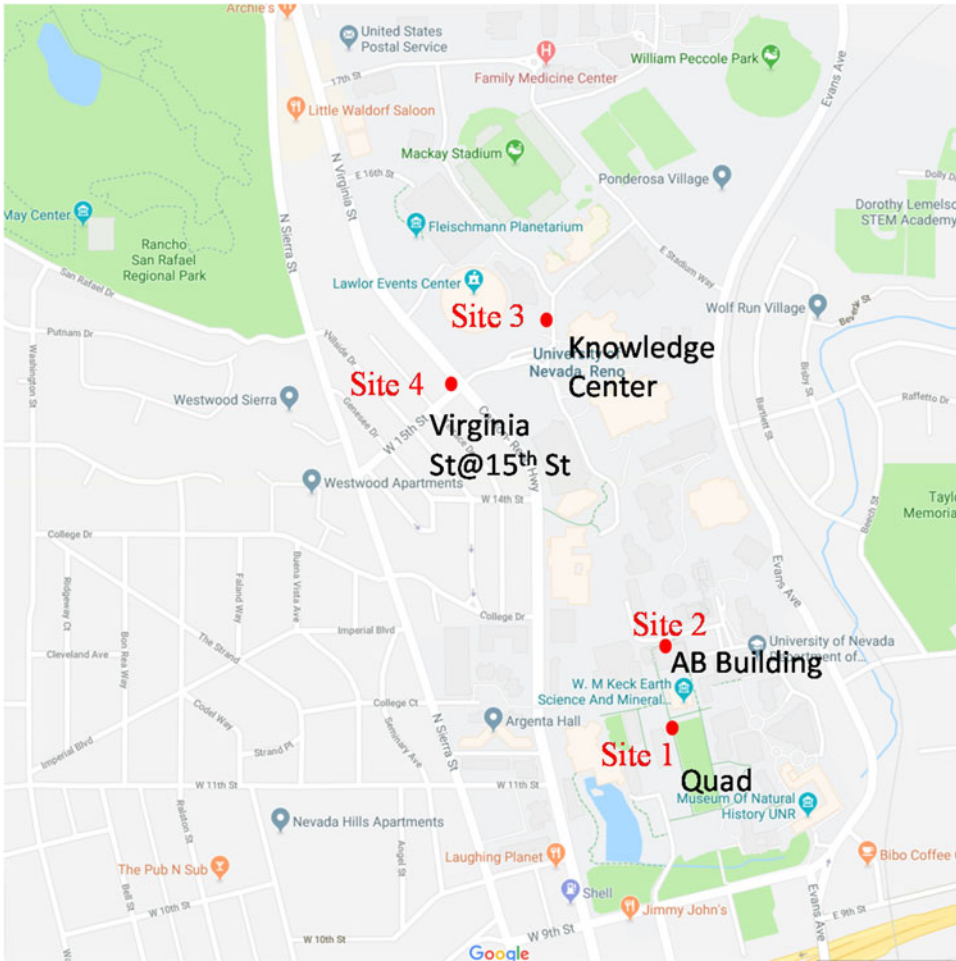


Figure 5. Map of the sites

Figure 8 shows the result of object clustering. The three road users were identified correctly from the roadside LiDAR data. Although there were some noises left in the space after background filtering. The density of the noise was low compared to road users. Therefore, those noises were cleaned up during the clustering step.

After object tracking, the trajectory of objects can be generated. Figure 9 shows an example of the trajectories in 2 hours generated by the object tracking algorithm at Site 3.

It is shown that the detailed trajectories of road users can be successfully generated using the proposed method. The whole data processing algorithm has been converted into a graphical user interface (GUI). Parts of the raw LiDAR data and the GUI are open to the public through the link: <https://nevada.box.com/s/x4056edthc93n2ecjmehzdmox889rjmg>.



Figure 6. Data collection sites

In the classification part, 251 vehicles, 145 skateboarders, 62 bicycles, and 320 pedestrians were manually marked. For stage 1, 70% of data in the database were used for training and the other 30% of the data were used for testing. Table 2 shows the results of classifications in the testing using KNN, SVM, RF, and NB. The confusion matrix shows that the RF can generate the results with the highest accuracy. The RF provided an improvement over bagged trees by a small tweak that decorrelated the trees. The RF can balance errors in data sets where the classes are imbalanced and work well for massive data sets with the large dimensionality.

Table 3 shows the confusion matrix of different methods in Stage 2. The RF also performed best among different methods. The overall accuracy is 89.17%. It was found that the skateboarders and the bicycles were more likely to be misclassified due to their similar speed distribution.

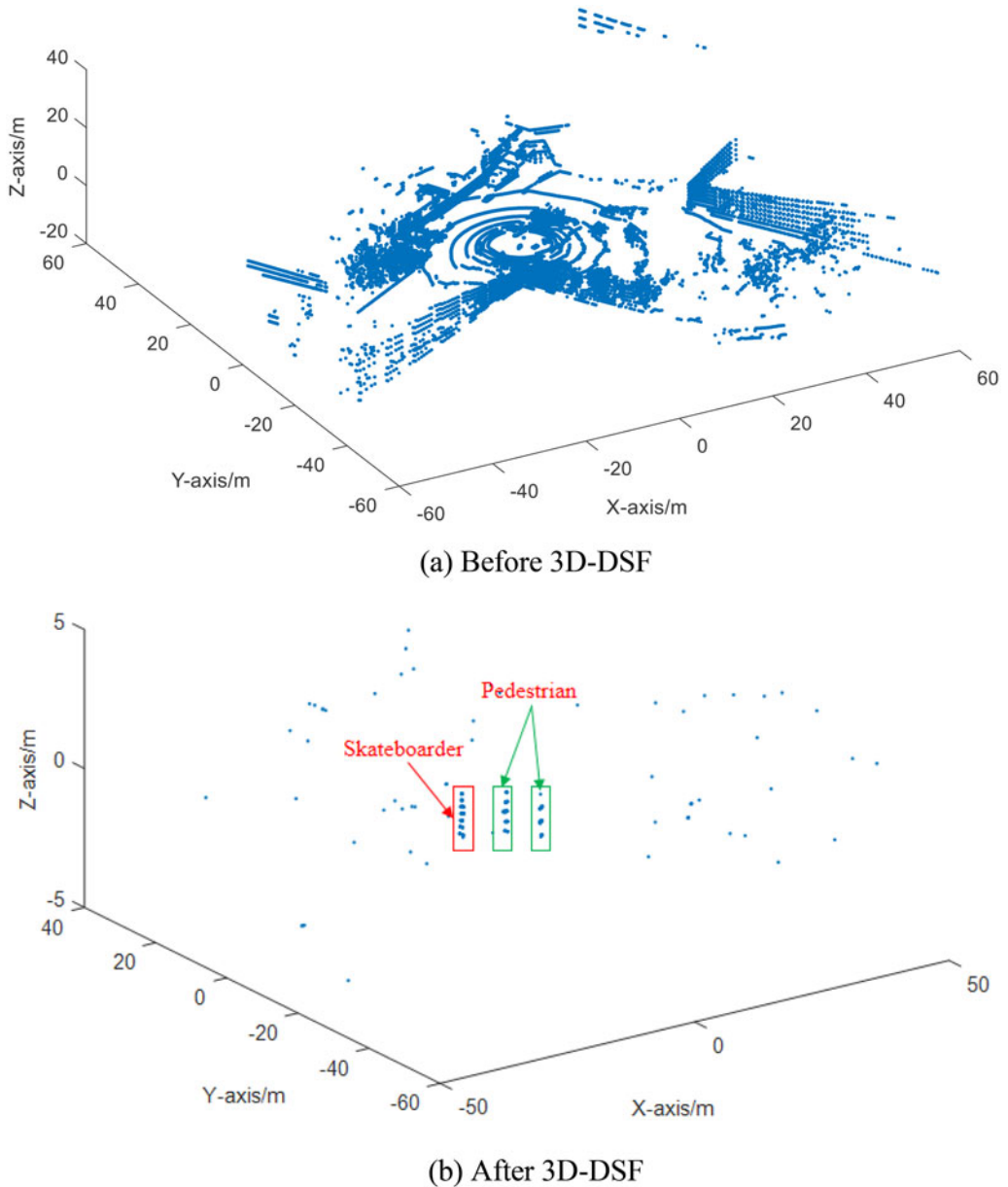


Figure 7. 3D-DSF at Site 2

4. Analysis of Skateboarder-Pedestrian conflicts

With the proposed algorithms, 359 skateboarders passing the pedestrian within 5 meters were extracted from three sites (except Site 4). A previous survey study showed that 71% of the respondents indicated that they would be more comfortable if the skateboarders gave them a 2- to 4-foot buffer and 40% of pedestrians indicated they would like eye contact with

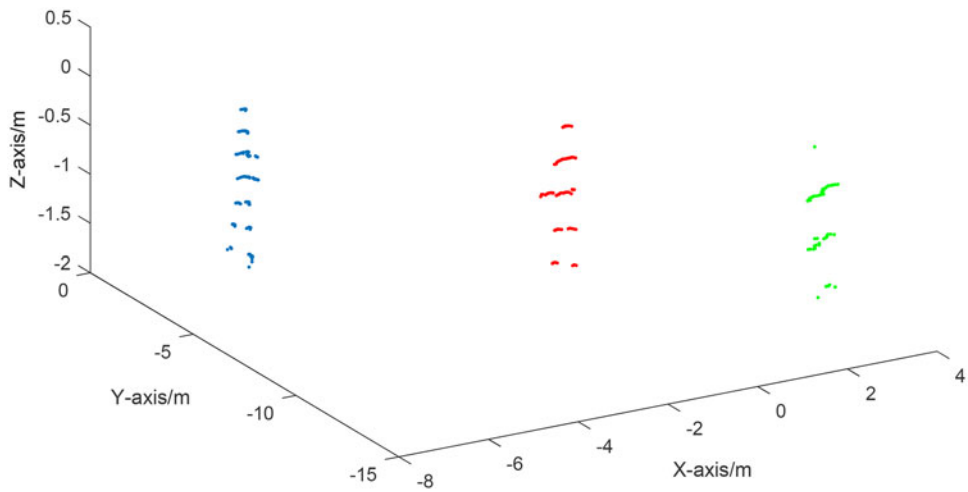


Figure 8. Clustering result

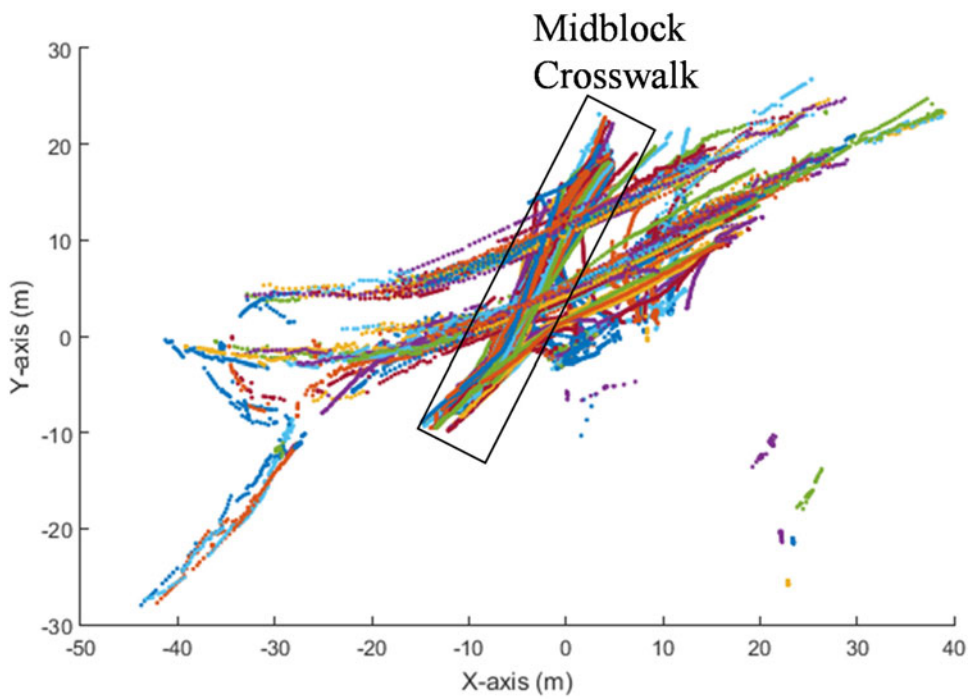


Figure 9. Trajectories of road users

skateboarders (Fang & Handy, 2017). Figure 10 shows the passing speed when the skateboarders have the shortest distance to pedestrians.

It was shown that 29.1% of skateboarders passed the pedestrians with a distance less than 1.2 m (4 ft). For those skateboarders passing the pedestrians with a distance shorter than 1.2 m (4 ft), 23.7% of them had a speed higher than 4 m/s. The relatively short distance to the pedestrians and the

Table 2. Confusion matrix

RF Predicted Class	Actual Class			NB Predicted Class	Actual Class		
	Nonvehicle	158	0		Nonvehicle	154	2
	Vehicle	0	75		Vehicle	4	73
KNN Predicted Class	Actual Class			SVM Predicted Class	Actual Class		
	Nonvehicle	154	5		Nonvehicle	155	2
	Vehicle	4	70		Vehicle	3	73

Note. RF = Random Forest; NB = Naive Bayes; KNN = K-Nearest Neighbors; SVM = Support Vector Machine

Table 3. Confusion matrix in Stage 2.

RF Predicted class	Actual class				NB Predicted class	Actual class			
	B	P	S			B	P	S	
	B	11	1	6		B	8	0	9
	P	0	94	2		P	0	92	4
KNN Predicted class	Actual class				SVM Predicted class	Actual class			
	B	P	S			B	P	S	
	B	8	3	5		B	8	0	10
	P	0	88	5		P	0	89	2
	S	10	5	33		S	10	7	31

Note. B = bicyclists; P = pedestrians; S = skateboarders; RF = Random Forest; NB = Naive Bayes; KNN = K-Nearest Neighbors; SVM = Support Vector Machine

high speed of skateboarders constituted the potential danger to the pedestrians or make the pedestrians uncomfortable. One important issue here is how to define a conflict. With the trajectories of pedestrians and skateboarders, it is possible to identify the skateboarder-pedestrian conflicts. The widely used indicator for surrogate safety measure is the time to collision (TTC). TTC is usually used to quantify and characterize the near crashes between vehicles. The limitation of TTC is that TTC assumes that drivers maintain their current speeds without the performance of evasive maneuvers (He, Qin, Liu, & Sayed, 2018). The authors have developed three indicators for the vehicle-pedestrian near-crash identification in a previous study (Wu, Xu, Zheng, & Tian, 2018). The three indicators can be revised to characterize skateboarder-pedestrian conflicts, as described in the following parts.

4.1. Time difference to the point of intersection

The time difference to the point of intersection (TDPI) was defined as “the time difference between a skateboarder and a pedestrian reaching the point of intersection in their trajectories”. Apparently, a longer TDPI represents a safer situation. Because 2.5 s was widely adopted as the standard driver reaction time (Wu, Xu, Zheng, & Tian, 2018), this paper considered 2.5 s as the threshold to determine a skateboarder-pedestrian conflict. Events with a TDPI less than 2.5 s were considered as the skateboarder-pedestrian conflicts.

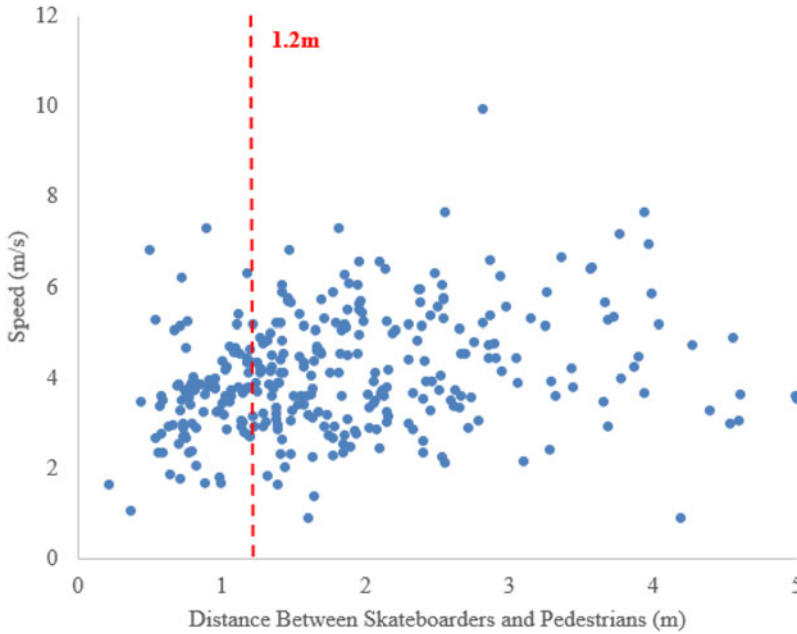


Figure 10. Passing speed with shortest distance to pedestrians

4.2. Shortest distance between skateboarder and pedestrian

The point of intersections may not exist between the trajectories of the skateboarder and the pedestrian, indicating the TDPI could not quantify those situations. The distance between skateboarder and pedestrian (DSP) was then developed. The DSP was defined as “the shortest distance between a skateboarder and a pedestrian at a timestamp in their trajectories”. We selected 1.2m as the threshold to determine the skateboarder-pedestrian conflict. Any events with the DSP less than 1.2m were considered as the skateboarder-pedestrian conflicts.

4.3. Speed-distance profile

The speed-distance profile can be used to represent the deceleration characteristics of the skateboarders. The skateboarder with a higher deceleration rate was dangerous to the pedestrian even if the DSP was longer than 1.2 m and the TDPI was longer than 2.5 s. However, there are no standards to guide the deceleration rate of the skateboarder. Therefore, this paper did not provide a recommendation for the skateboarder-pedestrian conflict identification using the speed-distance profile.

The final indicator for surrogate safety measure was determined by combing the DSP and the TDPI. A skateboarder-pedestrian conflict was identified if $\{TDPI < 2.5\text{ s or }DSP < 1.2\text{ m}\}$. It should be mentioned that

the recommended thresholds were based on the authors' best knowledge. The traffic engineers or researchers can definitively define their own thresholds for different purposes.

4.4. Recommended countermeasures

Some countermeasures are recommended to reduce the skateboarder-pedestrian conflicts. The countermeasures can be decomposed to three levels from highest to lowest: physical separation, physical enforcement, and mental enforcement. *Physical separation* refers to the strategies such as implementing no skateboarding zone or dedicated skateboarding lane under critical conflict areas, which can eliminate direct conflict between pedestrians and skateboarders. Although some campuses have limited space to reconstruct the facilities, in this regard, the median-level countermeasures can be used. The median-level countermeasures refer to physical enforcement, such as implementing stairs or bumps to forbid the skateboarding movement, it does not require to reconstructing a region but need some road attachments. These enforcements aim to deliver a message that no skateboarding movements are recommended in this area and thus reduce the skateboarder use. Even if we cannot put physical enforcement, mental enforcement can still be applied, such as painting red paints at critical conflict areas and blue or green paints at fewer conflict areas. Besides that, warning signs can be served as visual stimulation at the critical locations to warn skateboarders and pedestrians. Once the messages are delivered to either skateboarders or pedestrians, the danger would be effectively eliminated.

5. Conclusions

This research provided a systematic data processing algorithm to extract the skateboarder information from roadside LiDAR data automatically. The procedure includes background filtering, object clustering, object tracking, and classification. The detailed trajectories of the skateboarders can be obtained using the proposed procedure. The proposed method was evaluated using real-world collected data. The proposed procedure released the human work for counting the skateboarder from videos. **The testing results showed that the bicycle and skateboarder may be misclassified using the proposed method.** This was mainly caused by the uncertain speed of the skateboarder. For the VLP-16, due to the low resolution of points, the authors did not find an effective method to improve the classification between bicyclists and skateboarders. But if a high-resolution LiDAR, such as VLP-32c is applied, the shapes of bicyclists and skateboarders can be

clearer. Then the shape information can be further used to improve the accuracy of the classification. This paper recommends a level-based procedure to reinforce the safety regarding interactions between skateboarders and pedestrians. However, the effectiveness of these strategies requires further investigations.

ORCID

Jianqing Wu  <http://orcid.org/0000-0003-2844-6082>

References

- American Academy of Pediatrics: Committee on Injury and Poison Prevention. (2002). Skateboard injuries. *Pediatrics*, 109, 542–543.
- Beckwith, D., & Hunter-Zaworski, K. (1998). Passive pedestrian detection at unsignalized crossings. *Transportation Research Record: Journal of the Transportation Research Board*, 1636(1), 96–103. doi:10.3141/1636-16
- Chen, Z., Pears, N., Freeman, M., & Austin, J. (2009, November). Road vehicle classification using support vector machines. In 2009 IEEE International Conference on Intelligent Computing and Intelligent Systems (Vol. 4, pp. 214–218). IEEE.
- Carleton University. (2005). Bicycle, Rollerblade, Scooter and Skate Board Policy. Accessed electronically at http://www.carleton.ca/secretariat/policies/Bicycle_Rollerblade_Scooter_and_Skate_Board.html (accessed April 2009)
- Fang, K. (2013). Skateboarding as a legal travel mode: Review of regulations in California cities and college campuses. In: Proceedings of the 93rd Transportation Research Board Annual Meeting. Washington, DC.
- Fang, K., & Handy, S. (2017). Skate and die? The safety performance of skateboard travel: A look at injury data, fatality data, and rider behavior. *Journal of Transport & Health*, 7, 288–297. doi:10.1016/j.jth.2017.08.010
- Fang, K. (2015). Safety Indicators for Skateboarding on Transportation Facilities and as a Mode of Travel-A look at Enigmatic Injury, Fatality, and Incident Data. In TRB 94th Annual Meeting (No. 15-3800).
- Fang, K. (2014). Skateboarding Down the Street: Potential Factors Influencing the Decision to Skateboard as an Active Travel Mode-An Initial Exploration. In Transportation Research Board 93th Annual Meeting (No. 14-3431).
- Fountain, J. L., & Meyers, M. C. (1996). Skateboarding injuries. *Sports Medicine (Auckland, N.Z.)*, 22(6), 360–366. doi:10.2165/00007256-199622060-00004
- Hoogendoorn, S. P., Daamen, W., & Bovy, P. H. (2003, January). Extracting microscopic pedestrian characteristics from video data. In Transportation Research Board 92th Annual Meeting (pp. 1–15).
- He, Z., Qin, X., Liu, P., & Sayed, M. A. (2018). Assessing surrogate safety measures using a safety pilot model deployment dataset. *Transportation Research Record: Journal of the Transportation Research Board*, 2672(38), 1–11. doi:10.1177/0361198118790861
- Huang, H., Chin, H. C., & Haque, M. M. (2009). Empirical evaluation of alternative approaches in identifying crash hot spots: Naive Ranking, Empirical Bayes, Full Bayes Methods. *Transportation Research Record: Journal of the Transportation Research Board*, 2103(1), 32–41. doi:10.3141/2103-05
- Inoue, N., Barker, R., & Scott, D. A. (2009). Injury bulletin 105: Skateboard injury.

- Kothuri, S., Nordback, K., Schroepe, A., Phillips, T., & Figliozzi, M. (2017). Bicycle and pedestrian counts at signalized intersections using existing infrastructure: Opportunities and challenges. *Transportation Research Record: Journal of the Transportation Research Board*, 2644(1), 11–18. doi:10.3141/2644-02
- Lee, H., & Coifman, B. (2012). Side-fire lidar-based vehicle classification. *Transportation Research Record: Journal of the Transportation Research Board*, 2308(1), 173–183. doi:10.3141/2308-19
- Lustenberger, T., & Demetriades, D. (2017). Skateboarding injuries. In *Extreme sports medicine* (pp. 163–175). Cham: Springer.
- Li, Q., Zheng, N., & Cheng, H. (2004). Springrobot: A prototype autonomous vehicle and its algorithms for lane detection. *IEEE Transactions on Intelligent Transportation Systems*, 5(4), 300–308. doi:10.1109/TITS.2004.838220
- Milch, S., & Behrens, M. (2001). Pedestrian detection with radar and computer vision. Accessed April, 2019, from <http://citeseerx.ist.psu.edu/viewdoc/download?doi=10.1.1.20.9264&rep=rep1&type=pdf>.
- Malinovskiy, Y., Wu, Y. J., & Wang, Y. (2008). Video-based monitoring of pedestrian movements at signalized intersections. *Transportation Research Record: Journal of the Transportation Research Board*, 2073(1), 11–17. doi:10.3141/2073-02
- Nevada Traffic Crash Database. (2019). <https://www.nevadadot.com/safety/traffic-crash-data>. (accessed April
- Porter, B. E., Neto, I., Balk, I., & Jenkins, J. K. (2016). Investigating the effects of rectangular rapid flash beacons on pedestrian behavior and driver yielding on 25 mph streets: A quasi-experimental field study on a university campus. *Transportation Research Part F: Traffic Psychology and Behaviour*, 42, 509–521. doi:10.1016/j.trf.2016.05.004
- Ren, J., Chen, Y., Xin, L., Shi, J., Li, B., & Liu, Y. (2016). Detecting and positioning of traffic incidents via video-based analysis of traffic states in a road segment. *IET Intelligent Transport Systems*, 10(6), 428–437. doi:10.1049/iet-its.2015.0022
- Sun, Y., Xu, H., Wu, J., Zheng, J., & Dietrich, K. M. (2018). 3-D data processing to extract vehicle trajectories from roadside LiDAR data. *Transportation Research Record: Journal of the Transportation Research Board*, 2672(45), 14–22. doi:10.1177/0361198118775839
- Tan, M., Wang, B., Wu, Z., Wang, J., & Pan, G. (2016). Weakly supervised metric learning for traffic sign recognition in a LIDAR-equipped vehicle. *IEEE Transactions on Intelligent Transportation Systems*, 17(5), 1415–1427. doi:10.1109/TITS.2015.2506182
- University of Utah. (2009). Rule R805-1. Operating Regulations for Bicycles, Skateboards and Scooters. Accessed electronically at <http://www.rules.utah.gov/publicat/code/r805/r805-001.htm> (Accessed April 2019)
- University of California San Diego. (1997). Regulations concerning skateboarders and skating device. Accessed electronically at <http://adminrecords.ucsd.edu/PPM/docs/270-2.pdf> (accessed April 2019)
- University of Nevada Reno. (2015). Campus Master Plan 2015–2024 University Regional Center Plan. Accessed April, 2019, from https://www.unr.edu/Documents/business/NLI/Conferences/Sep%202015/The_University_of_Nevada_Reno_Master_Plan_Part_2.pdf.
- Wu, J., & Xu, H. (2018). The influence of road familiarity on distracted driving activities and driving operation using naturalistic driving study data. *Transportation Research Part F: Traffic Psychology and Behaviour*, 52, 75–85. doi:10.1016/j.trf.2017.11.018
- Wu, J., Xu, H., & Zheng, J. (2017, October). Automatic background filtering and lane identification with roadside LiDAR data. In *Intelligent Transportation Systems (ITSC), 2017 IEEE 20th International Conference on* (pp. 1–6). IEEE.

- Wu, J., Xu, H., Sun, Y., Zheng, J., & Yue, R. (2018). Automatic background filtering method for roadside LiDAR data. *Transportation Research Record*, 2672(45), 106–114.
- Wu, J., Tian, Y., Xu, H., Yue, R., Wang, A., & Song, X. (2019). Automatic ground points filtering of roadside LiDAR data using a channel-based filtering algorithm. *Optics & Laser Technology*, 115, 374–383. doi:[10.1016/j.optlastec.2019.02.039](https://doi.org/10.1016/j.optlastec.2019.02.039)
- Wu, J., Xu, H., & Zhao, J. (2019). Automatic lane identification using the roadside LiDAR Sensors. *IEEE Intelligent Transportation Systems Magazines*. doi:[10.1109/MITS.2018.2876559](https://doi.org/10.1109/MITS.2018.2876559)
- Wu, J., Xu, H., Zheng, Y., & Tian, Z. (2018). A novel method of vehicle-pedestrian near-crash identification with roadside LiDAR data. *Accident Analysis & Prevention*, 121, 238–249. doi:[10.1016/j.aap.2018.09.001](https://doi.org/10.1016/j.aap.2018.09.001)
- Wu, J. (2018). An automatic procedure for vehicle tracking with a roadside LiDAR sensor. Institute of Transportation Engineers. *ITE Journal*, 88(11), 32–37.
- Wu, J., Xu, H., Zhao, J., & Simpson, N. (2018). Autonomous Wildlife Crossing Detection Method with Roadside Lidar Sensors. In Transportation Research Board 97th Annual Meeting (No. 18-00500).
- Yang, B., Fang, L., & Li, J. (2013). Semi-automated extraction and delineation of 3D roads of street scene from mobile laser scanning point clouds. *ISPRS Journal of Photogrammetry and Remote Sensing*, 79, 80–93. doi:[10.1016/j.isprsjprs.2013.01.016](https://doi.org/10.1016/j.isprsjprs.2013.01.016)
- Zhao, J., Xu, H., Wu, D., & Liu, H. (2018). An Artificial Neural Network to Identify Pedestrians and Vehicles from Roadside 360-Degree LiDAR Data. In Transportation Research Board 97th Annual Meeting (No. 18-03129).
- Zhao, J., Xu, H., Liu, H., Wu, J., Zheng, Y., & Wu, D. (2019). Detection and tracking of pedestrians and vehicles using roadside LiDAR sensors. *Transportation Research Part C: Emerging Technologies*, 100, 68–87. doi:[10.1016/j.trc.2019.01.007](https://doi.org/10.1016/j.trc.2019.01.007)
- Zhao, J., Xu, H., Wu, J., Zheng, Y., & Liu, H. (2018). Trajectory tracking and prediction of pedestrian's crossing intention using roadside LiDAR. *IET Intelligent Transport Systems*, doi:[10.1049/iet-its.2018.5258](https://doi.org/10.1049/iet-its.2018.5258)
- Zheng, Y., Xu, H., Tian, Z., & Wu, J. (2018). Design and Implementation of the DSRC-Bluetooth Communication and Mobile Application with LiDAR Sensor. In Transportation Research Board 97th Annual Meeting (No. 18-00691).